Molecular Cancer Therapeutics

KIT-Dependent and KIT-Independent Genomic Heterogeneity of Resistance in Gastrointestinal Stromal Tumors — TORC1/2 Inhibition as Salvage Strategy

Thomas Mühlenberg[1,2], Julia Ketzer[1,2], Michael C. Heinrich[3], Susanne Grunewald[1,2], Adrian Marino-Enriquez[4], Marcel Trautmann[5], Wolfgang Hartmann[5], Eva Wardelmann[5], Jürgen Treckmann[6], Karl Worm[7], Stefanie Bertram[7], Thomas Herold[2,7], Hans-Ulrich Schildhaus[8], Hanno Glimm[2,9], Albrecht Stenzinger[2,10], Benedikt Brors[2,11], Peter Horak[2,12], Peter Hohenberger[13], Stefan Fröhling[2,12], Jonathan A. Fletcher[4], and Sebastian Bauer[1,2]

Abstract

Sporadic gastrointestinal stromal tumors (GIST), characterized by activating mutations of *KIT* or *PDGFRA*, favorably respond to KIT inhibitory treatment but eventually become resistant. The development of effective salvage treatments is complicated by the heterogeneity of *KIT* secondary resistance mutations. Recently, additional mutations that independently activate KIT-downstream signaling have been found in pretreated patients—adding further complexity to the scope of resistance. We collected genotyping data for *KIT* from tumor samples of pretreated GIST, providing a representative overview on the distribution and incidence of secondary *KIT* mutations ($n = 80$). Analyzing next-generation sequencing data of 109 GIST, we found that 18% carried mutations in KIT-downstream signaling intermediates (*NF1/2, PTEN, RAS, PIK3CA, TSC1/2, AKT, BRAF*) potentially mediating resistance to KIT inhibitors. Notably, we found no apparent other driver mutations in refractory cases that were analyzed by whole exome/genome sequencing (13/109). Using CRISPR/Cas9 methods, we generated a panel of GIST cell lines harboring mutations in *KIT, PTEN, KRAS, NF1*, and *TSC2*. We utilized this panel to evaluate sapanisertib, a novel mTOR kinase inhibitor, as a salvage strategy. Sapanisertib had potent antiproliferative effects in all cell lines, including those with KIT-downstream mutations. Combinations with KIT or MEK inhibitors completely abrogated GIST-survival signaling and displayed synergistic effects. Our isogenic cell line panel closely approximates the genetic heterogeneity of resistance observed in heavily pretreated patients with GIST. With the clinical development of novel, broad spectrum KIT inhibitors, emergence of non-KIT–related resistance may require combination treatments with inhibitors of KIT-downstream signaling such as mTOR or MEK.

Introduction

Gastrointestinal stromal tumors (GIST) are the most common sarcomas of the GI tract and are characterized by activating mutations of the KIT or PDGFRA receptor tyrosine kinases (1, 2). Most patients respond to the KIT/PDGFRA inhibitor imatinib (IM) but eventually progress due to secondary resistance mutations in *KIT* (3, 4). Second- and third-line KIT inhibitors have limited clinical benefit and only for a subset of patients (5–7). The development of effective salvage treatments is hampered by the heterogeneity of

[1]Department of Medical Oncology, Sarcoma Center, West German Cancer Center, University Duisburg-Essen, Medical School, Essen, Germany. [2]German Cancer Consortium (DKTK), Heidelberg, Germany. [3]Portland VA Health Care System, Knight Cancer Institute, Oregon Health and Science University, Portland, Oregon. [4]Department of Pathology, Brigham and Women's Hospital, Harvard Medical School, Boston, Massachusetts. [5]Gerhard Domagk Institute of Pathology, University Hospital Münster, Münster, Germany. [6]Department of Visceral and Transplant Surgery, Sarcoma Center, West German Cancer Center, University Duisburg-Essen, Medical School, Essen, Germany. [7]Institute of Pathology, University Hospital of Essen, University of Duisburg-Essen, Germany. [8]Institute of Pathology, Universitätsmedizin Göttingen, Göttingen, Germany. [9]Department of Translational Oncology, National Center for Tumor Diseases (NCT) Dresden, Dresden University Hospital, Dresden, Germany. [10]Institute of Pathology, Heidelberg University Hospital, Heidelberg, Germany. [11]Department of Applied Bioinformatics, German Cancer Research Center (DKFZ), Heidelberg University, Heidelberg, Germany. [12]Department of Translational Oncology, National Center for Tumor Diseases (NCT) Heidelberg, German Cancer Research Center (DKFZ), Heidelberg University Hospital, Heidelberg, Germany. [13]Mannheim, University Medical Center, Mannheim, Germany.

Note: Supplementary data for this article are available at Molecular Cancer Therapeutics Online (http://mct.aacrjournals.org/).

Corresponding Authors: Thomas Mühlenberg and Sebastian Bauer, University of Duisburg-Essen, Medical School, Hufelandstr. 55, Essen 45147, Germany. Phone: 49-201-723-2112; Fax: 49-201-723-3112; E-mail: thomas.muehlenberg@uk-essen.de; and Sebastian Bauer, Sebastian.bauer@uk-essen.de

Mol Cancer Ther 2019;18:1985–96

doi: 10.1158/1535-7163.MCT-18-1224

©2019 American Association for Cancer Research.

Downloaded from http://aacrjournals.org/mct/article-pdf/18/11/1985/1859957/1985.pdf by guest on 28 August 2022

resistance mutations in *KIT* often observed within a single patient (8–10).

The various *KIT* mutations in GIST activate the PI3K/AKT/mTOR and RAS/RAF/MAPK signaling pathways, and these same pathways are also activated in other GIST subtypes, even in so-called wild-type GIST (11). Recently, activating mutations in these signaling cascades, including *PI3K*, *KRAS*, *PTEN*, and *NF1*, have been shown to emerge in later treatment lines, representing resistance mechanisms that cannot likely be addressed using direct KIT-inhibition approaches (11, 12). Therefore, novel treatment strategies beyond the direct inhibition of KIT may become a crucial factor in GIST treatment in the near future. However, preclinical models recapitulating this heterogeneity of resistance, which would alleviate research towards this goal, do not exist yet. We used the Clustered Regularly Interspaced Short Palindromic Repeats/CRISPR-associated protein 9 (CRISPR/Cas9) system as a novel powerful tool to generate new GIST cell line models (13).

Inhibitors of KIT-downstream signaling intermediates (PI3K, mTOR, MEK) have been evaluated in GIST for several years but have not transitioned to advanced clinical development. Rapamycin-analogues targeting mTOR have only been examined in refractory GIST in combination with imatinib—which could not reverse imatinib resistance. However, next-generation mTOR kinase inhibitors have not yet been tested. Sapanisertib (INK0128, MLN0128, TAK-228) represents a novel class of ATP-competitive mTOR inhibitors, specifically inhibiting mTOR kinase in both mTOR complexes (mTORC) 1 and 2 (14). The compound has been shown to be a more potent inhibitor of mTOR signaling than rapamycin, one that can overcome intrinsic and acquired resistance to rapamycin, and is well tolerated *in vivo* and in early clinical trials (15–18).

Here, we sought to generate a GIST cell line panel comprising KIT-dependent and -independent mechanisms of resistance to current KIT inhibitors, approximating the clinical situation *in vitro*. We then utilized this panel to evaluate the efficacy of sapanisertib alone and in combination with KIT or MEK inhibition.

Materials and Methods

Patients

All patients were previously diagnosed as patients with GIST by routine pathologic review. In a retrospective study, we gathered all consecutive sequencing data available (Sanger + NGS) for patients with GIST who underwent routine molecular-pathology review in Essen. Furthermore we compiled panel NGS data of routine molecular-pathology review from sarcoma centers of Göttingen and Münster, Germany, and Portland, Oregon, as well as WES/WGS data from patients with GIST who participated in the DKTK MASTER program (19) in Heidelberg. Because of the nature of these data (i.e., anonymized molecular pathology review only, except for the DKTK MASTER cohort), no clinical data or sequencing raw data of these patients are available and no written informed consent could be requested or given. In this study, exclusively anonymized sequencing data were analyzed, allowing no inference to patient identity and medical history except for diagnosis. The study was approved by the institutional review board (IRB; ethics committee) of the Medical School of the University of Duisburg-Essen was conducted in accordance with the Declaration of Helsinki. For the DKTK MASTER cohort, all patients provided written informed consent under a protocol approved by the ethics committee of Heidelberg University, and the study was conducted in accordance with the Declaration of Helsinki.

Illumina—panel sequencing of tumor samples (63 patients)

Multiplex PCR and purification was performed with the GeneRead DNAseq Custom Panel V2, GeneRead DNAseq Panel PCR Kit V2 (QIAgen) and Agencourt AMPure XP Beads (Beckmann). A total amount of 44 ng DNA was used to perform multiplex PCR (4 primer pools with 11 ng each). Library preparation was performed using NEBNext Ultra DNA Library Prep Set for Illumina (New England Biolabs, NEB), according to the manufacturer's recommendations applying 24 different indices per run. The pooled library was sequenced on MiSeq (Illumina; 2×150 bases paired-end run) and analyzed by the Biomedical Genomics Workbench (CLC Bio; QIAgen). Within the CLC Cancer Research Workbench, demultiplexed paired-end sequencing data were mapped to human genome (version hg19). A local realignment was performed to reach better alignment quality, especially for regions with small insertions or deletions. All reads which were mapped outside of targeted-regions were deleted after the mapping process. In a filtering-step, all reference-variants and variants found in dbSNP common, 1,000 genome project and HapMap were deleted. An allele-frequency of minimum 2% and coverage of at least 100 mapped-reads were applied. Samples with less than 50% of mapped bases against hg19 were categorized as not analyzable. For deviations from this protocol, as performed for patients from Münster and Göttingen, and detailed information on sequencing panels see Supplementary Materials and Methods.

Ion Torrent—panel sequencing of tumor samples (33 patients)

Targeted sequence analysis was performed with a custom AmpliSeq panel (Life Technologies) that includes 24 genes (*AKT1*, *AKT2*, *AKT3*, *ATM*, *BRAF*, *CDKN2A*, *HRAS*, *KIT*, *KRAS*, *MAP2K1*, *NF1*, *NRAS*, *PDGFRA*, *PIK3CA*, *PTEN*, *PTPN11*, *RB1*, *SDHA*, *SDHAF1*, *SDHAF2*, *SDHB*, *SDHC*, *SDHD*, *TP53*). Sequencing was carried out on an Ion Torrent PGM instrument, and Torrent Suite Software v3.2 was used for sequence alignment and variant calling (20).

Whole exome/genome and RNA sequencing (13 patients)

DNA was extracted from 13 GIST samples from patients participating in the DKTK MASTER program (19) along with corresponding peripheral blood or adjacent normal tissue and subjected to whole exome/genome and RNA sequencing as described previously (21, 22). Reads were mapped to the 1,000 genomes phase II assembly of the human reference genome (NCBI build 37.1). Genome-sequencing data were aligned using Burrows-Wheeler Aligner, BWA (version 0.6.2 or 0.7.15). BAM files were sorted with SAMtools (version 0.1.19; ref. 23), and duplicates were marked with Picard tools (version 1.125). Single-nucleotide variants (SNV) and small insertions/deletions (indels) were analyzed using a previously reported bioinformatics workflow (24). Copy number variants (CNV) were extracted from the whole exome-sequencing samples with the help of CNVkit (version 0.8.3.dev0; ref. 25) and from the whole genome sequencing (WGS) data using our in-house CNV calling pipeline ACEseq (26). Structural variants were detected in whole exome sequencing (WES) data using CREST (27). All events were annotated with RefSeq genes using BEDTools (28). RNA-sequencing (RNA-Seq) data generated on the HiSeq 2500 platform were processed as

Downloaded from http://aacrjournals.org/mct/article-pdf/18/11/1985/1859957/1985.pdf by guest on 28 August 2022

described previously (24), RNA-Seq data generated on the HiSeq 4000 platform were aligned using STAR 2.5.1b (29). Relative RNA expression of 467 predefined cancer relevant genes, compared with median reads per kilobase million (RPKM) in a cohort of 149 diverse patients with cancer, is reported. Overexpressed genes with RPKM fold change >10 and *Z*-score >1 and underexpressed genes with RPKM fold change <0.25 and *Z*-score ←1 were evaluated. Sequencing data were deposited in the European Genome-phenome Archive under accession No. EGAS00001003405.

CRISPR/Cas9-mediated gene editing

To generate GIST-T1/V654A, GIST-T1/D816A, and GIST-T1/G12R suitable guide sequences targeting *KIT* exon 13 and 17, and *KRAS* exon 2, respectively, were identified using the online tool CRISPOR (www.crispor.org; ref. 30). For both *KIT* exons 2 adjacent guides were selected. A forward oligo containing the t7 RNA polymerase promoter sequence and the respective guide sequence, as well as a reverse oligo containing the generic single guide RNA sequence were purchased at MWG Eurofins. For guide RNA design, we used "FE-modified" sequences described by Chen and colleagues (31). The t7 RNA polymerase DNA template was generated by a fill-in PCR using Q5 high fidelity DNA polymerase (NEB), running 10 cycles of 62°C/20 seconds and 72°C/2 minutes. sgRNA was then transcribed with t7 RNA polymerase (NEB), according to manufacturer's instructions and precipitated by phenol/chlorophorm extraction, using standard protocols.

GIST-T1 cells were seeded in a T25 flask at low density and after 72 hours of growth cells were trypsinized, washed, and resuspended in electroporation buffer (Buffer SF; Lonza). A total of 10^5 cells were mixed with 0.5 to 0.7 μL Recombinant Cas9 (20 μmol/L; NEB), 0.5 to 0.7 μL *in vitro* transcribed sgRNA (20 μmol/L) per guide, and 0.5 to 0.7 μL single-stranded DNA template [ssODN (MWG Eurofins); 500 μmol/L], carrying the desired mutation to be introduced via the homology directed repair (HDR) pathway. Cells were electroporated using the program DN100 on the Amaxa Nucleofector 4D (Lonza). On the next day, the bulk cells were selected with IM 100 nmol/L until outgrowth of a resistant population was achieved. Sanger sequencing confirmed heterozygous mutations *KIT* V654A and D816A, and *KRAS* G12R, as well as silent mutations induced by the HDR templates. In the attempt to generate GIST-T1/G12R, we furthermore generated a subline harboring a heterozygous 23 bp deletion in *KRAS* (GIST-T1-KRAS) starting in exon 2, codon 9, causing a frameshift and premature stop codon within the exon. Interestingly, these cells showed strong activation of RAS downstream signaling (see Results). For a detailed list of sequences see Supplementary Materials and Methods.

CRISPR/Cas9-mediated gene knockout

For the generation of T1-PTEN and T1-TSC2, suitable guide sequences against *PTEN*, *TSC2*, with sticky-end overhangs were ordered from MWG Eurofins. Oligos were annealed, and cloned into the "lentiCRISPR v2" vector (Addgene Plasmid #52961), according to the published protocol (13). For PTEN knockout, the resulting plasmid was transfected by nucleofection as described previously. Twenty-four hours after transfection, cells were selected with puromycin 2 μmol/L for 96 hours. For TSC2 knockout, the plasmid was transduced after lentiviral Packaging, according to standard protocols. Five days after transfection, cells were selected with puromycin 2 μmol/L for 96 hours. Cells were then further selected with IM 100 nmol/L until outgrowth of a resistant population. For NF1 knockout cell (T1-NF1), lentiviral constructs encoding SpCas9 (pXPR_BRD001; Broad Institute) and an anti-NF1 guide RNA (pXPR_BRD003) were transduced by 2 consecutive lentiviral infections, followed by 1 week of 2 μmol/L of puromycin selection, and further selection with IM 100 nmol/L until outgrowth of a resistant population. Knockout was confirmed by Western blot analysis and next-generation sequencing. For a detailed list sequences, see Supplementary Materials and Methods.

Cell lines

Apart from the cell lines described previously, further IM-sensitive (GIST-T1, GIST882, GIST430) and IM-resistant (GIST430/654, GIST-T1-D816E, GIST48B) cell lines were studied. GIST-T1 and GIST882 were established from human, untreated, metastatic GISTs, and carry primary-activating mutations in exons 11(V560_Y578del) and 13 (K642E), respectively. GIST430/654 was established from a GIST that had progressed, after initial clinical response during IM therapy and harbors a primary activating mutation in exon 11 (51 bp del V560-Y578) and secondary resistance mutation in exon 13 (V654A). GIST430 is an IM-sensitive subline, with only the primary *KIT* exon 11 (51 bp del V560-Y578) mutation but no secondary resistance mutation, derived from the same GIST culture as the GIST430/654 line. GIST48B, despite retaining the activating *KIT* mutation in all cells, expresses *KIT* transcript and protein at essentially undetectable levels. GIST-T1 was established by Takahiro Taguchi (Kochi University, Kochi, Japan). GIST882 were cultured in RPMI1640 containing 15% FBS and 1% Pen/Strep (Gibco). All other cell lines were cultured in IMDM containing 10% FBS and 1% Pen/Strep. Cell lines are regularly authenticated by sequencing of endogenous mutations in *KIT*, confirmation of KIT expression, and response to KIT inhibitor treatment. In the course of this study, all cell lines were regularly tested for mycoplasma contamination by PCR and by MycoAlert Mycoplasma Detection Kit (Lonza).

Reagents and antibodies

Sapanisertib, imatinib, sunitinib, ponatinib, trametinib, and everolimus (RAD001) were purchased form Selleck chemicals. A primary polyclonal rabbit antibody against KIT was purchased from Dako. A monoclonal mouse antibody against β-actin was purchased from Sigma. All other primary and secondary antibodies used in this study were purchased from Cell Signaling Technologies.

Western blot analysis

Cells were plated in 6-well plates and on the next day treated with different inhibitors or vehicle control. After 24 hours of treatment, lysis buffer (1% NP-40, 50 mmol/L Tris-HCl pH 8.0, 100 mmol/L sodium fluoride, 30 mmol/L sodium pyrophosphate, 2 mmol/L sodium molybdate, 5 mmol/L EDTA and 2 mmol/L sodium vanadate; freshly adding 0.1% 10 mg/mL aprotinin and leupeptin as well as 1% 100 mmol/L PMSF and 200 mmol/L sodium vanadate) was added, and cells were scraped off and then lysed while rotating for 1 hour at 4°C. Lysates were centrifuged at 4°C for 30 minutes at 18,000rcf and protein concentration was determined using the Bio-Rad Protein Assay (Bio-Rad Laboratories). Protein concentration was adjusted to 2 μg/μL (if not otherwise specified), SDS-loading buffer (0.5 M

Downloaded from http://aacrjournals.org/mct/article-pdf/18/11/1985/1859957/1985.pdf by guest on 28 August 2022

Tris-HCl pH 6.7, 10% SDS, 2.5% DTT, 50% glycerol, and 0.05% bromophenol blue) was added and lysates were incubated for 5 minutes at 95°C. Equal amounts of protein (30 μg per lane, if not otherwise specified) were separated on SDS-PAGE Gels (NuPAGE 4%–12%; Life Technologies) and blotted onto nitrocellulose-membranes (GE Healthcare/Amersham-Biosciences). After blocking with Net-G buffer (1.5 M NaCl, 50 mmol/L EDTA, 500 mmol/L Tris, 0.5% Tween 20, and 0.4% gelatine), membranes were incubated at 4°C overnight with the respective primary antibody. After washing (Net-G), membranes were incubated for 2 hours at room temperature with a secondary antibody (in Net-G) and washed again. Changes in protein expression and phosphorylation as visualized by chemiluminescence were captured and quantified using a FUJI LAS3000 system with Science Lab 2001 ImageGauge 4.0 software (Fujifilm Medial Systems). Usually 2 to 4 gels/membranes were prepared from the same experiment/lysates, to enable clean stains of proteins with similar or nearby molecular weight as well as stains of total proteins and their phosphorylated counterparts. Membranes were consecutively stained with different antibodies of different molecular weights. β-Actin served as loading control for each membrane and a representative stain is shown.

Sulforhodamin B assay

Cell viability was evaluated by Sulforhodamin B (SRB; Sigma-Aldrich) assay after 72 hours of treatment, as previously described (32). Cells were treated with increasing concentrations of DMSO-dissolved compounds, sapanisertib, trametinib, imatinib, sunitinib, regorafenib, ponatinib. Mean values were normalized to DMSO-solvent control and the mean standard error was calculated. All experiments were carried out in triplicate/quadruplicate cultures at least twice and a representative example is shown.

Dose-combination studies

For dose-finding experiments, 1,000 cells/well were seeded in white 384-well plates (Greiner) using the Multidrop (Thermo Fisher Scientific) and allowed to attach overnight. Respective compounds were added in duplicates or triplicates using the digital dispenser Tecan D300e, and normalized to identical solvent volumes. After 72 hours Cell Titer Glo (Promega) reagent was added according to manufacturer's instructions. Luminescence was measured on the Tecan Spark M10. The combinatorial index (CI) was calculated according to the method by Chou–Talalay (33), using CalcuSyn Software (BioSoft). For confirmation, the most effective combinations were then evaluated in triplicates in 96-well plates using the SRB assay.

Results

Patients with GIST display heterogeneity of resistance to KIT inhibition

First we reviewed the in-house sequencing data bases for mutations in patients with GIST found during routine clinical testing in our centers. We thus compiled a cohort of 80 patients with secondary resistance mutations in *KIT*, 11 of which displayed more than one such mutation in the particular examined biopsies (Fig. 1). Most of these were point mutations in exon 13 (V654A) or exon 17 (involving codons 820, 822, or 823). However, we also found less common mutations in amino acids D677, C809, and S840.

Next, we queried our next-generation sequencing patient data ($n = 109$) for mutations in KIT downstream effectors, such as *NF1*,

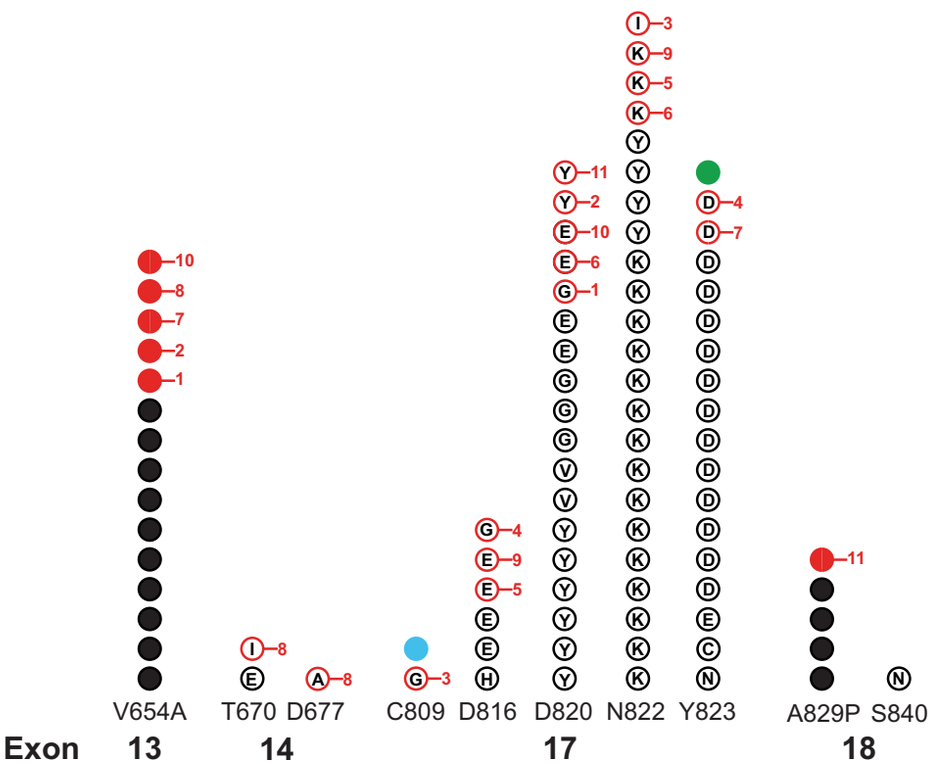

Figure 1.
Resistance mutations in KIT found in patients with GIST. Distribution of secondary *KIT* mutations in exons 13, 14, 17, and 18 (mixed sanger and NGS; $n = 80$). Black = point mutation; red = patients ($n = 11$) presented >1 resistance mutation in the same or in subsequent biopsies; blue = frame shift mutation with STOP at c.813; green = in-frame InDel (823_G827delIns5). Letters indicate the respective amino acid change.

Downloaded from http://aacrjournals.org/mct/article-pdf/18/11/1985/1859957/1985.pdf by guest on 28 August 2022

Table 1. Non-*KIT* mutations, with potential for causing KIT-inhibitor resistance

Patient	Gene	AA-change	AF (%)	KIT/PDGFRA mutation
1	*AKT3*	F27I	13	PDGFRA – D842V + V658A
2	*BRAF*	V600E	60	WT
3	*BRAF*	V600E	32	WT
4	*KRAS*	G13D	36	KIT – e11 + N822K
5	*PIK3CA*	H1065Y	33	KIT – e11 + N822K
6	*PIK3CA*	H1047R	21	KIT – e11
7	*PIK3CA*	H1047R	81	KIT – e11
8[a]	*NF1*	M1981V	5	KIT – e11 + Y823E
9[a]	*NF1*	I719fs	32	KIT – e11 + D820Y + A829P
10	*PTEN*	I122S	78	KIT – e11
11	*TSC1*	E479del	46	PDGFRA – D842V
12	*TSC2*	A1719T	58	PDGFRA – D842V

NOTE: Next-generation sequencing data (Illumina panel, Ion Torrent panel, WES, WGS) was analyzed for mutations in *KIT*-downstream signaling intermediates. Total NGS patients, $n = 109$.

Abbreviations: AA, amino acid; AF, allelic frequency; LOH, loss of heterozygosity.

[a]Patient also appears in Table 2.

N/H/KRAS, BRAF, PTEN, PIK3CA, AKT, and *TSC1/2*. We found that a subset of patients (18%; 20/109) displayed such downstream mutations, potentially causing resistance to KIT/PDGFRA-inhibitors (Tables 1 and 2). Notably, 10% (3/31) of patients with primary *PDGFRA* mutations displayed mutations in downstream signaling intermediates, indicating a similar incidence of these events as in *KIT* mutated GIST. Except for the *BRAF*-mutated cases, all patients with downstream effector mutations also displayed activating mutations in *KIT* or *PDGFRA*, most *of which were accompanied by* secondary resistance mutations (13/18; Tables 1 and 2).

Thirteen mostly heavily pretreated (median treatment lines = 4) patients with TKI-resistant GIST were recruited into the DKTK MASTER molecular stratification program (19) in which tumors are analyzed by whole exome/genome and RNA sequencing to identify clinically actionable aberrations. In these datasets, we identified primarily alterations in genes that are involved in the PI3K or MAPK signaling pathways (Table 2). Notably, no driver mutations apart from KIT and its downstream pathways were detected (Supplementary Fig. S1). Furthermore, RNA-Seq data revealed mostly lineage-specific markers among the highest ranking transcripts (*KIT*, *PDGFRA*, *ETV1*; Table 2).

Novel cell line panel approximates genetic heterogeneity of patients with GIST

To expand our panel of models recapitulating the heterogeneity of resistance in GIST, we applied CRISPR/Cas9 mediated gene editing and knockout. We thus induced heterozygous point mutations of *KIT* in exon 13 (V654A) and exon 17 (D816A), respectively, in addition to the endogenous primary exon 11 mutation in GIST-T1. As expected, these cells displayed a much higher resistance to IM as well as an inhibitory profile towards the approved second- and third-line KIT-inhibitors sunitinib (SU) and regorafenib (RE), matching their respective secondary mutations (Table 3).

To investigate the effect of oncogenic mutations in KIT-downstream signaling intermediates on KIT-inhibitor sensitivity, we generated further GIST-T1 sublines: T1/G12R-HOM/HET harboring homozygous and heterozygous G12R mutations in *KRAS*, respectively, as well as T1-KRAS with a heterozygous KRAS deletion (see Materials and Methods; Fig. 2). The cell lines T1-PTEN, T1-TSC2, and T1-NF1 carry homozygous knockout of PTEN, TSC2, and NF1, respectively. Although TSC2- and NF1-deficient cells were completely resistant to KIT inhibition, cells with loss of PTEN displayed some sensitivity to IM treatment, which still efficiently inhibits KIT-dependent MEK signaling (Table 3). However, these cells would still continue to grow, albeit slower, at high IM concentrations (10 μmol/L; Supplementary Fig. S2). Interestingly the heterozygous mutation of $KRAS^{G12R}$ did not cause a notable increase in tolerance to KIT inhibition, whereas cells carrying homozygous $KRAS^{G12R}$ were, similar to T1-KRAS, partly resistant (Supplementary Fig. S3). As depicted in Table 3, cell lines harboring mutations in *KIT* or its downstream signaling intermediates are highly resistant to all currently approved GIST treatments.

Sapanisertib has antiproliferative effects in IM-sensitive and IM-resistant GIST cell lines

We then sought to evaluate the therapeutic potential of KIT-downstream inhibition using the mTOR kinase inhibitor sapanisertib. In cell viability assays after 3 days of treatment, sapanisertib displayed IC_{50} values between 20 nmol/L (GIST430/654) and 70 nmol/L (T1-G12R; Fig. 3A). Sensitivity towards sapanisertib was independent of secondary mutations, sensitivity to IM, and KIT expression (GIST48B). Strikingly, cell lines harboring KIT-independent resistance mutations in *KRAS, PTEN, TSC2*, and *NF1* were similarly sensitive to sapanisertib treatment.

Sapanisertib efficiently abrogates mTORC1/2 signaling

To elucidate the effects of sapanisertib on intracellular signaling, we conducted Western blot experiments in GIST cell lines of different origins. We observed a dose-dependent inhibition of ribosomal protein S6 phosphorylation (pS6; as marker for mTOR activation) starting at 1 to 5 nmol/L with complete inhibition at 50 to 100 nmol/L in all cell lines (Fig. 2B). Notably, in this concentration range sapanisertib mediated inhibition of mTORC2 led to a strong inhibition of AKT phosphorylation (pAKT), followed by loss of 4E-BP1 phosphorylation (p4E-BP1). In contrast, 20 nmol/L everolimus (RAD001), while also potently inhibiting pS6, did not inhibit pAKT or p4e-BP1, but instead increased their phosphorylation levels. Interestingly, sapanisertib treatment, especially at higher concentrations, led to a dose-dependent increase of ERK1/2 phosphorylation (pERK; Fig. 2B).

Cotreatment inhibits feedback induction of MEK/ERK signaling

mTOR inhibition alone appeared to leave the cells with an escape route via MEK/ERK-driven survival, as indicated by induction of pERK1/2 (Fig. 2B). Therefore, we combined sapanisertib either with KIT-inhibition or with the clinical MEK inhibitor trametinib (Fig. 3). Combinations with KIT inhibitors displayed the strongest effects in cell lines with KIT-downstream mutations, which was to be expected as GIST-T1-PTEN and KRAS-mutated sublines displayed residual sensitivity to IM alone (Table 3; Supplementary Figs. S2 and S3). Strikingly, in GIST–T1–TSC2, combination of sapanisertib and IM completely abrogated S6 and 4E-BP1 phosphorylation, even at sapanisertib doses as low as 10 nmol/L, whereas IM alone did not inhibit S6 and 4E-BP1 phosphorylation. These cells displayed reduced baseline KIT-expression which increased after IM treatment (Figs. 2 and 3). Combinations of sapanisertib with trametinib completely abrogated both KIT-downstream signaling axes in all investigated cell lines.

Downloaded from http://aacrjournals.org/mct/article-pdf/18/11/1985/1859957/1985.pdf by guest on 28 August 2022

Table 2. Genetic and transcriptional abberations identified by WES/WGS and RNA-Seq

Patient	Pretreatment	KIT primary (exon)	KIT secondary	NF1	NF2	PTEN	TSC1/2	RNA-expression (HIGH: fold change > 10 + z-score > 1; LOW: fold change < 0.25 + z-score < −1)
1	IM; SU; RE; Pazo	11	A829P	—	—	LOH	LOH (TSC2)	HIGH: KIT; PTCH1; FOXL2; EPHA3; ETV1; FGFR1; LMO2; JAK3; AFF3; SOCS1; PDGFRA LOW: SDC4
2[a]	IM; RE	11	Y823E	M1981V	LOH	—	—	HIGH: FOXL2; KIT; TLX1; NTRK2; EPHA3; USP6; PTCH1; GPC3; MYB; LMO2; WNK2; DDR2; ETV1 LOW: SMAD4; SDC4; DDR1
3	IM; SU	11	A829P	—	LOH	—	—	HIGH: KIT; NTRK2; GPC3; NRG3; CARD11; ETV1; AFF3; MYB; EPHA3; BCL2; DDR2; PBX1; ZBTB16 LOW: PLK2; PTPRJ; NRAS; RAD54B; RB1; SDC4; DDR1; RUNX1
4	IM; SU; IM+BYL719; RE; Pona; SU+Sirolimus; Pazo; Cabozantinib	11	V654A T670I D677A	—	LOH	—	—	HIGH: KIT; RSPO2; ETV1; EPHA3; PTCH1; AFF3; LMO2; DDR2; SOCS1; FGFR1; CARD11 LOW: STL; RUNX1; DDR1; SDC4
5	IM; SU; Pazo; RE; Pona; Nilo	11	D816E N822K	LOH	LOH	LOH	LOH (TSC1)	HIGH: RSPO2; FOXL2; HOXA11; ETV1; IL2 LOW: EWSR1; EP300; MAF; SUFU; BRD4; ELF4; MAP2K1; TPM4; MSN; ERC1; TRAF7; GAK; STIL; TOP1; CIC; EXT1; SET; TPM3; CUX1; PTPRK; ATP1A1; CLIP1; SMARCB1; KIF5B; PPFIBP1; RUNX1; SMARCA4; PTPRJ; NF2; SRC; MKL1; THRAP3; NOTCH2; WHSC1; DCTN1; IDH2; NOTCH1; TAF15; BCR; LASP1; SDC4; HIP1; DDR1; MYH9
6	IM; SU; RE; Pazo; SU+Sirolimus	11	V654A D820E	—	—	—	—	HIGH: CD79B; FEV; IDO2; HIST1H3B LOW: MLLT6; BCL9; FANCE; NT5C2; KRAS; TPM3; SF3B1; TCEA1; RIT1; MAF; RAB35; CCDC6; ARID1A; CDC73; XPO1; NUMA1; GAK; TCF12; KDM6A; MED12; SET; CBL; CBLB; CRTC1; CDKN1B; RB1; USP11; MYH9; MLLT1; NIN; CHEK1; KTN1; RASA1; BCL10; MRE11A; SMARCA4; FBXO11; ATRX; RAD21; PMS1; TOP1; KIF5B; TPM4; SUZ12; ELL; CIC; STIL; RNF2; SFPQ; KDM5C; GOPC; STAG2; FIP1L1; PHF6; SRC; ATF1; TCF3; DEK; PTPN12; HDAC2; CBFB; RALGDS; MSH2; FUBP1; DDR1; PLK1; AURKA; RAD51AP1; MLF1; CDK1; PSIP1; NOTCH1; ELF4; RUNX1; HIST1H4I
7[a]	IM; SU	9	D820Y A829P	I719fs	LOH	—	LOH (TSC1)	HIGH: KIT; FOXL2; EPHA3; ETV1; CARD11; MYB; AFF3; SOCS1; ZNF521; LMO2; JAK3 LOW: HIP1; PPFIBP1; PTPRK; STIL; PTPRF; SDC4; STL; DDR1
8	IM; SU; RE; Pona; Nilo; SU+Sirolimus; Pazo	11	R634L D820G	—	—	—	LOH (TSC1)	HIGH: KIT; HOXA11; MYCN; ETV1; AFF3; LMO2; FGF2; FGFR1 LOW: HIP1; ELF4; NOTCH1; PTPRJ; PLK2; RUNX1; MAF; SDC4; FOXO1
9	IM; Masitinib; SU; IM; RE	11	Y823C	—	LOH	—	—	HIGH: KIT; HOXA11; HOXA9; NRG3; ETV1; HLF; NRG2; AFF3; FGF1; WNK2; LMO2; DDR2; CDH11 LOW: SDC4; RUNX1
10	IM; IM (800); SU; Nilo; RE; Pazo; SU+Sirolimus	9	D816E	—	LOH	—	—	HIGH: RSPO2; ALK; KIT; HOXA13; FOXL2; NRG2; HOXA11; EPHA3; SOCS1; ETV1; HOXA9; AFF3; ZNF521
				—		—	—	LOW: HIP1; RUNX1; SDC4
11	IM	18		—	—	—	—	n.a.
12	IM; SU	11	D820Y	—	LOH	—	—	n.a.
13	IM; SU; RE; IM	9		—	—	—	—	HIGH: KIT; CD79B; EPHA3; ETV1; LMO2; ERG; HOXA11; SOCS1; JAK3; NRG4; BRIP1; MLLT11; BCL2 LOW: STL; RUNX1; SDC4; DDR1

NOTE: Thirteen patients were analyzed (WES/WGS) for mutations in KIT-downstream signaling intermediates. A total of 11 of 13 patients were additionally analyzed by RNA-Seq and the transcripts with highest and lowest abundance are shown, ordered from highest to lowest fold change, compared with control.

Abbreviations: IM, imatinib; LOH, loss of heterozygosity; n.a., not available; Nilo, nilotinib; Pazo, pazopanib; PO, ponatinib; RE, regorafenib; SU, sunitinib.

[a]Patient also appears in Table 1.

Downloaded from http://aacrjournals.org/mct/article-pdf/18/11/1985/1859957/1985.pdf by guest on 28 August 2022

Table 3. Antiproliferative effects of sapanisertib compared with current KIT inhibitors

	IC_{50} (nmol/L)			
Cell line	**IM**	**SU**	**RE**	**Sap**
GIST-T1	35	9	30	35
T1-G12R-HOM	n.r.	n.r.	1,000	70
T1-G12R-HET	30	25	90	50
T1-KRAS	n.r.	1,500	450	45
T1-NF1	n.r.	6,000	1,100	50
T1-PTEN	150	25	150	50
T1-TSC2	n.r.	n.r.	900	35
T1-V654A	850	30	300	25
T1-D816A	700	5,000	150	50
T1-D816E	850	3,000	200	45
GIST430	25	5	15	35
GIST430/654	250	25	50	20
GIST882	300	75	350	40
GIST48B	n.r.	6,000	10,000	50

NOTE: IC_{50} values from cell viability assays (SRB) after 72 hours of treatment with increasing doses of imatinib (IM), sunitinib (SU), regorafenib (RE), and sapanisertib (Sap). n.r., not reached.

Combinational treatment with KIT or MEK inhibitors displays synergistic effects

To further elucidate the potential of combinational treatment, we next conducted multidose combination proliferation experiments with sapanisertib, combined with either KIT-inhibition or trametinib. Cells were treated with 5 to 100 nmol/L of each inhibitor and with each possible combination of 2 drugs. We then calculated the CI for each combination according to the Chou–Talalay method, which describes synergy at CI < 1, additivity at CI = 1, and antagonism at CI > 1. We found that concentrations of sapanisertib between 25 and 100 nmol/L yielded the strongest combinatorial effects in all cell lines (Table 4). In most cell lines, combinations with IM yielded at best moderate additive effects (CI, 0.5–0.58) at low concentrations of IM (50–200 nmol/L). However, in TSC2-deficient cells, the combination displayed a strong synergy signified by the lowest CI-value of 0.26 (Table 4). In the sublines harboring secondary *KIT* mutations (V654A and D816A), cells were treated with sunitinib and ponatinib, respectively. These combinations also had moderate synergistic effects.

Combinations of sapanisertib and trametinib showed strong synergistic effects in all examined cell lines (lowest CI values: 0.126–0.37; Table 3; Supplementary Fig. S3). Notably, the lowest CI-value overall of 0.126 was obtained in TSC2-deficient cells when sapanisertib 25 nmol/L was combined with trametinib 200 nmol/L. However, even at lower concentrations of trametinib 25 and 50 nmol/L, the combination with sapanisertib 25 nmol/L had strong synergistic effects (CI-values 0.33 and 0.19, respectively; Supplementary Fig. S3). All calculated CI-values, as well as the results of the cytotoxicity experiments they were generated from are depicted in Supplementary Fig. S3.

Discussion

Activating mutations of *KIT* or *PDGFRA* are the oncogenic hallmarks of GIST that lead to ligand-independent downstream activation of the PI3K and RAS/RAF/MAPK signaling cascades (2, 34). Inhibition of KIT by imatinib abrogates KIT phosphorylation and consequently signaling through these pathways. Although most GISTs exhibit long-lasting responses to KIT-inhibitor therapy, the majority of patients eventually progress. Secondary mutations in *KIT* have been identified as the main mechanism of resistance in resection specimens of patients failing imatinib (6). This is accompanied by reactivation of PI3K and RAS/RAF/MAPK signaling. Notably, these 2 pathways seem to be required for GIST homeostasis and proliferation regardless of the presence of *KIT* or *PDGFRA* mutations—thus defining crucial tissue-specific pathways. Therefore, in a broader sense, GIST could be defined not by KIT activation itself, but rather by conjoined activation of its downstream signaling intermediates (11).

Therapeutic success in GIST is therefore not defined only by successful inhibition of KIT but, in extension, by abrogation of KIT downstream signaling. Sustained therapeutic KIT inhibition is confounded by the heterogeneity of secondary KIT IM-resistance mutations, whereas activity of therapies targeting KIT downstream signaling might depend on the types of mutations activating these downstream pathways. Very recently, genomic activation of KIT-downstream pathways has even been observed in treatment-naïve GIST, further underscoring the clinical relevance of KIT-independent mutations within these pathways (12, 35).

In an international collaborative effort, we interrogated the pathology databases of several GIST centers, and thus compiled a representative spectrum and incidence of secondary *KIT* mutations in a large cohort of TKI-refractory GIST. Interestingly, we found a lower incidence of exon 14 mutations compared with reports from the early 2000s (6, 7). This may be reflective of the availability of additional KIT inhibitors in recent years, which effectively inhibit the exon 14 gatekeeper mutations. Also, there could be technical bias, as *KIT* exon 14 was not sequenced in the early years of routine pathologic diagnosis in all centers, these patients may have been falsely classified as not carrying a secondary *KIT* mutation. Our data indicate the need for more potent KIT inhibitors, with activity against the full spectrum of resistance mutations. Of note, latest generation KIT inhibitors show broader and more specific inhibitory profiles (36, 37), although no drug has yet been shown to be equally and universally potent against all *KIT* mutations.

Recently, next-generation panel sequencing was introduced into routine pathologic analysis in many centers, covering genes whose activation or loss could confer resistance apart from secondary *KIT* mutations. We were thus able show the incidence of non-*KIT* mutations in random samples of TKI-resistant GIST specimens sent for genotyping. In a fraction larger than expected, these comprise KIT-downstream signaling intermediates in the PI3K/AKT/mTOR and RAS/RAF/MAPK pathways. Of note, most mutations of tumor suppressor genes appeared heterozygous in this cohort, which might result from homozygous mutations present in only a subset of the neoplastic cells, which would not be surprising given that these were generally secondary KIT/PDGFRA-inhibitor resistance mutations. Another possibility is that inactivating mutations in the remaining tumor suppressor allele were often present but undetected, which can occur in the instance of large indels or promoter-region mutations. We also cannot exclude the possibility that some inactivations were truly heterozygous, and that haploinsufficiency in this context is biologically meaningful.

Although, this "tertiary resistance" has rarely been reported yet our results underscore the importance and functional relevance of mutations in these pathways (11, 12). We speculate that these mutations are frequently not tested for or even not added to routine pathology reports, despite the availiability of the data, for example, when only KIT sequencing is requested. Given the

Downloaded from http://aacrjournals.org/mct/article-pdf/18/11/1985/1859957/1985.pdf by guest on 28 August 2022

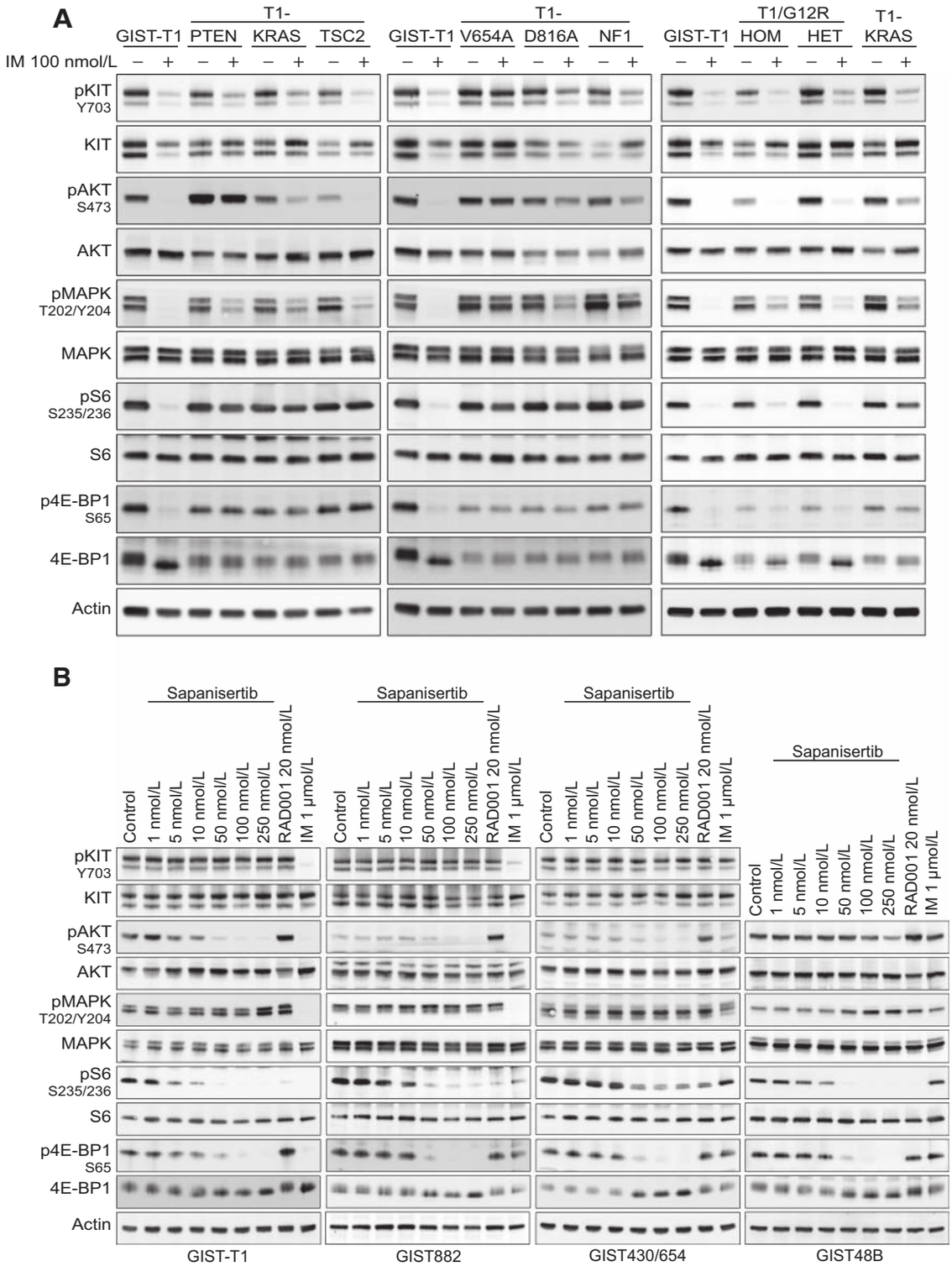

Figure 2.

Western blot analyses of the novel isogenic GIST-T1 subline panel and other GIST cell lines. **A,** Effects of 24 hours IM 100 nmol/L treatment of KIT and KIT-dependent signaling in the novel GIST-T1 subline panel compared with parental GIST-T1. For direct comparison between T1/G12R-HOM/HET and T1-KRAS, T1-KRAS appears twice in this panel (first and last column), and cell lysates were prepared from 2 independent experiments. **B,** Sapanisertib dose–response studies in IM-sensitive and IM-resistant GIST cell lines after 24 hours of treatment in comparison to RAD001 (everolimus) and IM.

Downloaded from http://aacrjournals.org/mct/article-pdf/18/11/1985/1859957/1985.pdf by guest on 28 August 2022

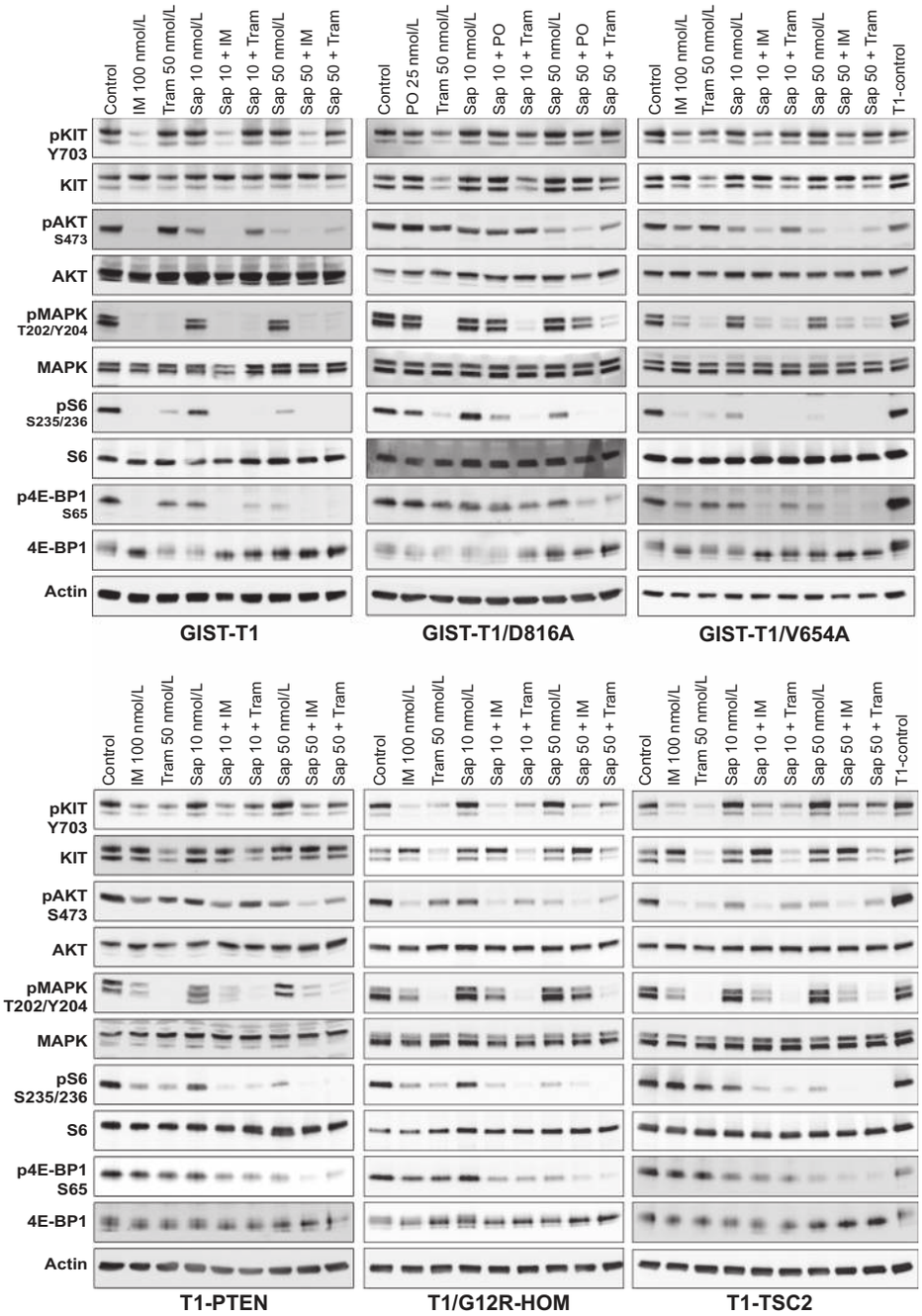

Figure 3.
Western blot analyses of sapanisertib (Sap) in combination with trametinib and KIT inhibitors. In IM-sensitive GIST-T1 and IM-resistant GIST-T1 sublines, sapanisertib was combined with either MEK inhibition (trametinib) or KIT inhibition (imatinib, ponatinib) for 24 hours, and effects on KIT-related signaling were examined.

advent of broader KIT inhibitors, we expect that these novel mechanisms represent a clinically relevant cause of treatment resistance, as GIST cells are crucially depending on the PI3K and RAS/RAF–MAPK pathways. Future studies, using plasma sequencing with sequencing panels optimized for GIST will most likely reveal these mutations to be more common than previously expected.

To our surprise, comprehensive DNA and RNA sequencing in a subset of patients revealed no other apparent driver mutations that may have replaced KIT signaling as the dominant oncogenic pathway. This finding underscores the requirement for concomitant activation of PI3K and MAPK signaling GIST cell homeostasis. Inhibiting KIT downstream signaling may therefore prove to be a necessary, effective, and actionable strategy.

To help validate our hypotheses, we expanded our panel of GIST cell lines, to model mechanisms of the complex heterogeneity observed in the clinic. Using CRISPR/Cas9 methods, we induced specific point mutations in *KIT*, and *KRAS* and thus show for the first time that precise genomic editing in GIST cell lines is possible and is a valuable tool to generate clinically relevant models. Up to now, KIT-inhibitor studies for GIST were often conducted in Ba/F3 cells, lacking the GIST-specific cellular

Downloaded from http://aacrjournals.org/mct/article-pdf/18/11/1985/1859957/1985.pdf by guest on 28 August 2022

Table 4. CIs obtained from combination studies

	Sap + IM				Sap + Tram			
Cell line	**Lowest CI**	**Sap (nmol/L)**	**IM (nmol/L)**	**Fa**	**Lowest CI**	**Sap (nmol/L)**	**Tram (nmol/L)**	**Fa**
GIST-T1	0.52	25	50	0.72	0.19	25	25	0.65
T1/G12R-HOM	0.56	25	50	0.44	0.27	50	50	0.66
T1-KRAS	0.5	50	100	0.55	0.37	50	50	0.62
T1-PTEN	0.5	50	200	0.74	0.27	25	50	0.67
T1-NF1	0.58	50	100	0.54	0.13	25	100	0.69
T1-TSC2	0.26	50	200	0.77	0.13	25	200	0.79
T1/V654A	0.45	25	50[a]	0.71	0.19	50	25	0.71
T1/D816A	0.37	50	25[a]	0.75	0.21	25	50	0.66

NOTE: In combination studies, increasing doses of IM or Tram (12.5–200 nmol/L) were combined with 25, 50, or 100 nmol/L or sapanisertib. After 3 days, cell survival was measured by SRB and the fraction affected (Fa) and CI were calculated. For each cell line, the best combination as signified by the lowest CI value is displayed.
Abbreviation: CI, combinatorial index.
[a]For T1-V654A and T1-D816A, IM was substituted with SU and ponatinib, respectively.

background (38). In fact, perturbations of GIST-specific KIT-downstream signaling are probably not optimally modelled in those systems. To date, virtually no *in vitro* studies have been conducted in GIST harboring mutations in signaling intermediates downstream of KIT (39).

Furthermore, our newly generated cell lines will not only enable improved inhibitor research but may also yield relevant insights into GIST biology. Of note, we observed that KIT expression decreased in GIST-T1 sublines with mutations in *KRAS*, *NF1*, and *TSC2*, but not *PTEN*. Inhibition of mTOR upon sapanisertib treatment subsequently increased the levels of total KIT (Figs. 2 and 3). Especially in cells lacking TSC2, this reactivation also reinstated KIT-dependence and thus sensitivity to IM treatment (Fig. 3; Table 4). These findings indicate that KIT-independent mutations may supplant the role of KIT and may impact KIT expression levels. Loss of KIT has been occasionally observed in clinical specimens and also in GIST cell lines grown *in vitro* (40). In this context, our modified sublines may serve as informative models to better understand the feedback regulation of KIT by its main intracellular signaling pathways. We were furthermore surprised to find that, at least in our GIST-T1–derived cell line model, the heterozygous mutation of $KRAS^{G12R}$ was not able to confer KIT-inhibitor resistance. We assume that GIST-T1 is particularly dependent on the RAS/RAF/MEK signal so that the activation of a single allele does not compensate for the complete block of the upstream KIT-dependent signal. In other cancers with KRAS-mediated mechanisms of TKI-resistance, very little data are published on the zygosity of secondary mutations. Notably, Serrano and colleagues recently reported a $KRAS^{G12R}$ mutated resistant GIST clone bearing a hemizygous mutation (12).

Targeting mTOR has been a strategy in clinical trials based on the observation that PI3K-activation is a signaling hallmark in GIST regardless of the presence of secondary resistance mutations (41). However, clinical success may have been hampered by pharmacologic interactions as well as the selection of a refractory treatment setting, in which imatinib was unlikely to inhibit clones with secondary resistance mutations (42). For imatinib-resistant clones, mTOR inhibition (everolimus) alone is most likely not sufficient to fully control tumor growth and it may require a combination with a broader KIT-inhibitor or with inhibitors of MEK. Based on preclinical findings in GIST (43), imatinib in combination with MEK is currently being tested in the clinic (NCT01991379). Another approach based on the *in vivo* studies by van Looy and colleagues (44) recently looked at the combination of imatinib and the PI3K-inhibitor Alpelisib (BYL719). Unfortunately, the results of this study are not yet available.

In contrast to everolimus, sapanisertib inhibits not only mTORC1, but also mTORC2 (45). This distinct inhibitory profile, causing a strong decrease of AKT- as well as 4E-BP1-phosphorylation, may yield superior clinical efficacy. Notably, compared with other rapalogs, which also inhibit mTORC2, sapanisertib has been shown to only cause grade 1 and 2 hyperglycemia and only in a subset of patients (17, 46). We now report that sapanisertib has strong antiproliferative effects in IM-sensitive and IM-resistant cell lines, including KIT-negative GIST. As Slotkin and colleagues have shown sapanisertib has antitumor effects in a panel of bone and soft tissue sarcoma cell lines and xenograft models (47). In their study, cell lines displaying *in vitro* IC_{50} values similar to the ones described herein were also inhibited *in vivo* at a dose of 1 mg/kg/day. Furthermore, effective concentrations for this drug against the IM-resistant GIST models are well within the range of clinically achievable plasma levels (17, 18). Currently sapanisertib is investigated in several clinical phase II trials, in entities including lung cancer, acute lymphoblastic leukemia and soft tissue sarcomas (clinicaltrials.gov).

However, RAS/RAF/MAPK signaling, unperturbed by sapanisertib, is similarly important for GIST cell proliferation and survival (41). Combinations of sapanisertib with approved KIT inhibitors display moderate synergistic effects and may represent a feasible clinical strategy, which warrants further investigation. To date, MEK inhibitors show clinical toxicity profiles requiring careful management in combination therapies (48, 49). We found strong synergistic effects when combining sapanisertib with trametinib, which was to be expected as this combination inhibits the 2 major routes of GIST proliferation and survival. These strong combinational effects might allow for dose reduction of one or both drugs which may reduce side effects and thus become more attractive to patients, especially to those with non-*KIT* resistance mutations. Although it is possible that the particular prototypic compounds or their combinations selected for our in vitro studies may display *in vivo* toxicity, we are convinced that inhibition of the 2 major oncogenic signaling axes in GIST will prove to be a clinically feasible treatment option. We speculate that in a disease exceptionally dependent on these pathways, such as GIST, the therapeutic window of such drug combinations may be even more favorable than in other cancers.

In summary, our data strongly underscore the need for comprehensive sequencing of *KIT* as well as of KIT-related signaling molecules that may contribute to KIT-inhibitor resistance in GIST. With the advent of more potent KIT-inhibitory molecules we hypothesize that mutations of genes coding for KIT-downstream signaling intermediates will become more prevalent. Future

Downloaded from http://aacrjournals.org/mct/article-pdf/18/11/1985/1859957/1985.pdf by guest on 28 August 2022

treatment strategies, both in untreated and pretreated GIST may benefit from integrating potent inhibitors of these pathways. The novel cell lines presented herein may provide meaningful models for the validation of such new drug combinations.

Disclosure of Potential Conflicts of Interest

M.C. Heinrich reports receiving a commercial research grant from Blueprint Medicines and Deciphera Pharmaceuticals; has ownership interest (including patents) in MolecularMD and Novartis; has consultant/advisory board relationship with Blueprint Medicines Deciphera Pharmaceuticals; and has provided expert testimony for Novartis. E. Wardelmann reports receiving other commercial research support from Nanobiotix, Novartis, Lilly, PharmaMar, and Menarini; and has consultant/advisory board relationship with New Oncology, Milestone, and Bayer. H. Glimm reports receiving other commercial research support from CRC. Albrecht Stenzinger has consultant/advisory board relationship with Astra Zeneca, Novartis, BMS, Bayer, Takeda, Illumina, and Thermo Fisher Scientific. S. Bauer reports having received commercial research support from Novartis (institutional), Blueprint Medicines (institutional support), and Incyte (institutional support); acted as consultant/advisor for Blueprint Medicines, Deciphera, Exelixis, Novartis, ADC-Therapeutics, Nanobiotix, and Lilly; and received honoraria for certified CME presentations (Pfizer, Bayer, Novartis). No potential conflicts of interest were disclosed by the other authors.

Authors' Contributions

Conception and design: T. Mühlenberg, S. Bauer

Development of methodology: T. Mühlenberg, M.C. Heinrich, J.A. Fletcher, S. Bauer

Acquisition of data (provided animals, acquired and managed patients, provided facilities, etc.): T. Mühlenberg, M.C. Heinrich, S. Grunewald, A. Marino-Enriquez, M. Trautmann, W. Hartmann, E. Wardelmann, J. Treckmann, K. Worm, H.-U. Schildhaus, H. Glimm, A. Stenzinger, P. Hohenberger, S. Fröhling, J.A. Fletcher, S. Bauer

Analysis and interpretation of data (e.g., statistical analysis, biostatistics, computational analysis): T. Mühlenberg, J. Ketzer, M.C. Heinrich, S. Grunewald, A. Marino-Enriquez, J. Treckmann, K. Worm, T. Herold, A. Stenzinger, B. Brors, P. Horak, S. Fröhling, S. Bauer

Writing, review, and/or revision of the manuscript: T. Mühlenberg, J. Ketzer, M.C. Heinrich, A. Marino-Enriquez, W. Hartmann, E. Wardelmann, J. Treckmann, S. Bertram, T. Herold, H.-U. Schildhaus, A. Stenzinger, P. Horak, P. Hohenberger, S. Fröhling, J.A. Fletcher, S. Bauer

Administrative, technical, or material support (i.e., reporting or organizing data, constructing databases): J. Ketzer, M. Trautmann, E. Wardelmann, P. Hohenberger, S. Fröhling, S. Bauer

Study supervision: T. Mühlenberg, H. Glimm, S. Bauer

Acknowledgments

The authors sincerely thank Miriam Christoff for the expert technical assistance. This work was supported by funds from the fundraising event "Sarkomtour" (www.sarkomtour.de; S. Bauer). Whole-exome/genome and RNA sequencing was funded by the DKTK Joint Funding Program (to S. Fröhling). Further support was received from the GIST Cancer Research Fund (to M.C. Heinrich) and VA Merit Review Grant (2I01BX000338-05, to M.C. Heinrich).

The costs of publication of this article were defrayed in part by the payment of page charges. This article must therefore be hereby marked *advertisement* in accordance with 18 U.S.C. Section 1734 solely to indicate this fact.

Received October 26, 2018; revised January 21, 2019; accepted July 8, 2019; published first July 15, 2019.

References

1. Hirota S, Isozaki K, Moriyama Y, Hashimoto K, Nishida T, Ishiguro S, et al. Gain-of-function mutations of c-kit in human gastrointestinal stromal tumors. Science 1998;279:577–80.
2. Heinrich MC, Corless CL, Duensing A, McGreevey L, Chen CJ, Joseph N, et al. PDGFRA activating mutations in gastrointestinal stromal tumors. Science 2003;299:708–10.
3. Verweij J, Casali PG, Zalcberg J, LeCesne A, Reichardt P, Blay JY, et al. Progression-free survival in gastrointestinal stromal tumours with high-dose imatinib: randomised trial. Lancet 2004;364:1127–34.
4. Blanke CD, Demetri GD, Von Mehren M, Heinrich MC, Eisenberg B, Fletcher JA, et al. Long-term results from a randomized phase II trial of standard- versus higher-dose imatinib mesylate for patients with unresectable or metastatic gastrointestinal stromal tumors expressing KIT. J Clin Oncol 2008;26:620–5.
5. Demetri GD, Reichardt P, Kang YK, Blay JY, Rutkowski P, Gelderblom H, et al. Efficacy and safety of regorafenib for advanced gastrointestinal stromal tumours after failure of imatinib and sunitinib (GRID): an international, multicentre, randomised, placebo-controlled, phase 3 trial. Lancet 2012;381:295–302.
6. Heinrich MC, Corless CL, Blanke CD, Demetri GD, Joensuu H, Roberts PJ, et al. Molecular correlates of imatinib resistance in gastrointestinal stromal tumors. J Clin Oncol 2006;24:4764–74.
7. Heinrich MC, Maki RG, Corless CL, Antonescu CR, Harlow A, Griffith D, et al. Primary and secondary kinase genotypes correlate with the biological and clinical activity of sunitinib in imatinib-resistant gastrointestinal stromal tumor. J Clin Oncol 2008;26:5352–9.
8. Wardelmann E, Merkelbach-Bruse S, Pauls K, Thomas N, Schildhaus HU, Heinicke T, et al. Polyclonal evolution of multiple secondary KIT mutations in gastrointestinal stromal tumors under treatment with imatinib mesylate. Clin Cancer Res 2006;12:1743–9.
9. Agaimy A, Wunsch PH, Hofstaedter F, Blaszyk H, Rummele P, Gaumann A, et al. Minute gastric sclerosing stromal tumors (GIST tumorlets) are common in adults and frequently show c-KIT mutations. Am J Surg Pathol 2007;31:113–20.
10. Kawanowa K, Sakuma Y, Sakurai S, Hishima T, Iwasaki Y, Saito K, et al. High incidence of microscopic gastrointestinal stromal tumors in the stomach. Hum Pathol 2006;37:1527–35.
11. Li B, Garcia CS, Marino-Enriquez A, Grunewald S, Wang Y, Bahri N, et al. Conjoined hyperactivation of the RAS and PI3K pathways in advanced GIST. J Clin Oncol 2016;34(15_suppl):e22520.
12. Serrano C, Wang Y, Marino-Enriquez A, Lee JC, Ravegnini G, Morgan JA, et al. KRAS and KIT gatekeeper mutations confer polyclonal primary imatinib resistance in GI stromal tumors: relevance of concomitant phosphatidylinositol 3-kinase/AKT dysregulation. J Clin Oncol 2015;33:e93–6.
13. Ran FA, Hsu PD, Wright J, Agarwala V, Scott DA, Zhang F. Genome engineering using the CRISPR-Cas9 system. Nat Protoc 2013;8:2281–308.
14. Hsieh AC, Liu Y, Edlind MP, Ingolia NT, Janes MR, Sher A, et al. The translational landscape of mTOR signalling steers cancer initiation and metastasis. Nature 2012;485:55–61.
15. Hassan B, Akcakanat A, Sangai T, Evans KW, Adkins F, Eterovic AK, et al. Catalytic mTOR inhibitors can overcome intrinsic and acquired resistance to allosteric mTOR inhibitors. Oncotarget 2014;5:8544–57.
16. Sun SY. mTOR kinase inhibitors as potential cancer therapeutic drugs. Cancer Lett 2013;340:1–8.
17. Ghobrial IM, Siegel DS, Vij R, Berdeja JG, Richardson PG, Neuwirth R, et al. TAK-228 (formerly MLN0128), an investigational oral dual TORC1/2 inhibitor: a phase I dose escalation study in patients with relapsed or refractory multiple myeloma, non-Hodgkin lymphoma, or Waldenstrom's macroglobulinemia. Am J Hematol 2016;91:400–5.
18. Burris HA 3rd, Kurkjian CD, Hart L, Pant S, Murphy PB, Jones SF, et al. TAK-228 (formerly MLN0128), an investigational dual TORC1/2 inhibitor plus paclitaxel, with/without trastuzumab, in patients with advanced solid malignancies. Cancer Chemother Pharmacol 2017;80:261–73.
19. Horak P, Klink B, Heining C, Groschel S, Hutter B, Frohlich M, et al. Precision oncology based on omics data: the NCT Heidelberg experience. Int J Cancer 2017;141:877–86.

Downloaded from http://aacrjournals.org/mct/article-pdf/18/11/1985/1859957/1985.pdf by guest on 28 August 2022

20. Beadling C, Neff TL, Heinrich MC, Rhodes K, Thornton M, Leamon J, et al. Combining highly multiplexed PCR with semiconductor-based sequencing for rapid cancer genotyping. J Mol Diagn 2013;15:171–6.
21. Heining C, Horak P, Uhrig S, Codo PL, Klink B, Hutter B, et al. NRG1 fusions in KRAS wild-type pancreatic cancer. Cancer Discov 2018;8:1087–95.
22. Chudasama P, Mughal SS, Sanders MA, Hubschmann D, Chung I, Deeg KI, et al. Integrative genomic and transcriptomic analysis of leiomyosarcoma. Nat Commun 2018;9:144.
23. Li H, Handsaker B, Wysoker A, Fennell T, Ruan J, Homer N, et al. The sequence alignment/map format and SAMtools. Bioinformatics 2009;25: 2078–9.
24. Kordes M, Roring M, Heining C, Braun S, Hutter B, Richter D, et al. Cooperation of BRAF(F595L) and mutant HRAS in histiocytic sarcoma provides new insights into oncogenic BRAF signaling. Leukemia 2016;30: 937–46.
25. Talevich E, Shain AH, Botton T, Bastian BC. CNVkit: genome-wide copy number detection and visualization from targeted DNA sequencing. PLoS Comput Biol 2016;12:e1004873.
26. Kleinheinz K, Bludau I, Huebschmann D, Heinold M, Kensche P, Gu Z, et al. ACEseq - allele specific copy number estimation from whole genome sequencing. bioRxiv 2017. doi: https://doi.org/10.1101/210807.
27. Wang J, Mullighan CG, Easton J, Roberts S, Heatley SL, Ma J, et al. CREST maps somatic structural variation in cancer genomes with base-pair resolution. Nat Methods 2011;8:652–4.
28. Quinlan AR, Hall IM. BEDTools: a flexible suite of utilities for comparing genomic features. Bioinformatics 2010;26:841–2.
29. Dobin A, Davis CA, Schlesinger F, Drenkow J, Zaleski C, Jha S, et al. STAR: ultrafast universal RNA-seq aligner. Bioinformatics 2013;29:15–21.
30. Haeussler M, Schonig K, Eckert H, Eschstruth A, Mianne J, Renaud JB, et al. Evaluation of off-target and on-target scoring algorithms and integration into the guide RNA selection tool CRISPOR. Genome Biol 2016;17:148.
31. Chen B, Gilbert LA, Cimini BA, Schnitzbauer J, Zhang W, Li GW, et al. Dynamic imaging of genomic loci in living human cells by an optimized CRISPR/Cas system. Cell 2013;155:1479–91.
32. Muhlenberg T, Grunewald S, Treckmann J, Podleska L, Schuler M, Fletcher JA, et al. Inhibition of KIT-glycosylation by 2-deoxyglucose abrogates KIT-signaling and combination with ABT-263 synergistically induces apoptosis in gastrointestinal stromal tumor. PLoS One 2015;10:e0120531.
33. Chou TC, Talalay P. Quantitative analysis of dose-effect relationships: the combined effects of multiple drugs or enzyme inhibitors. Adv Enzyme Regul 1984;22:27–55.
34. Hirota S, Nishida T, Isozaki K, Taniguchi M, Nakamura J, Okazaki T, et al. Gain-of-function mutation at the extracellular domain of KIT in gastrointestinal stromal tumours. J Pathol 2001;193:505–10.
35. Lasota J, Kowalik A, Felisiak-Golabek A, Zieba S, Wang ZF, Miettinen M. New mechanisms of mTOR pathway activation in KIT-mutant malignant GISTs. Appl Immunohistochem Mol Morphol 2019;27:54–8.
36. Evans EK, Gardino AK, Kim JL, Hodous BL, Shutes A, Davis A, et al. A precision therapy against cancers driven by KIT/PDGFRA mutations. Sci Transl Med 2017;9. doi: 10.1126/scitranslmed.aao1690.
37. Janku F, Razak ARA, Gordon MS, Brooks DG, Flynn DL, Kaufman M, et al. Pharmacokinetic-driven phase I study of DCC-2618 a pan-KIT and PDGFR inhibitor in patients (pts) with gastrointestinal stromal tumor (GIST) and other solid tumors. J Clin Oncol 2017;35(15_Suppl):2515.
38. Garner AP, Gozgit JM, Anjum R, Vodala S, Schrock A, Zhou T, et al. Ponatinib inhibits polyclonal drug-resistant KIT oncoproteins and shows therapeutic potential in heavily pretreated gastrointestinal stromal tumor (GIST) patients. Clin Cancer Res 2014;20:5745–55.
39. Marino-Enriquez A, Li B, Bahri N, Lauria A, Wang Y, Fletcher JA. NF1 loss modulates cellular fitness in KIT-mutant gastrointestinal stromal tumor (GIST). [abstract]. In: Proceedings of the 107th Annual Meeting of the American Association for Cancer Research; 2016 Apr 16–20; New Orleans, LA. Philadelphia (PA): AACR; Cancer Res 2016; 76(14 Suppl). Abstract nr 290.
40. Mearadji A, den Bakker MA, van Geel AN, Eggermont AM, Sleijfer S, Verweij J, et al. Decrease of CD117 expression as possible prognostic marker for recurrence in the resected specimen after imatinib treatment in patients with initially unresectable gastrointestinal stromal tumors: a clinicopathological analysis. Anticancer Drugs 2008;19:607–12.
41. Bauer S, Duensing A, Demetri GD, Fletcher JA. KIT oncogenic signaling mechanisms in imatinib-resistant gastrointestinal stromal tumor: PI3-kinase/AKT is a crucial survival pathway. Oncogene 2007;26: 7560–8.
42. Schoffski P, Reichardt P, Blay JY, Dumez H, Morgan JA, Ray-Coquard I, et al. A phase I-II study of everolimus (RAD001) in combination with imatinib in patients with imatinib-resistant gastrointestinal stromal tumors. Ann Oncol 2010;21:1990–8.
43. Ran L, Sirota I, Cao Z, Murphy D, Chen Y, Shukla S, et al. Combined inhibition of MAP kinase and KIT signaling synergistically destabilizes ETV1 and suppresses GIST tumor growth. Cancer Discov 2015;5: 304–15.
44. Van Looy T, Wozniak A, Floris G, Sciot R, Li H, Wellens J, et al. Phosphoinositide 3-kinase inhibitors combined with imatinib in patient-derived xenograft models of gastrointestinal stromal tumors: rationale and efficacy. Clin Cancer Res 2014;20:6071–82.
45. Maiso P, Liu Y, Morgan B, Azab AK, Ren P, Martin MB, et al. Defining the role of TORC1/2 in multiple myeloma. Blood 2011;118:6860–70.
46. Sivendran S, Agarwal N, Gartrell B, Ying J, Boucher KM, Choueiri TK, et al. Metabolic complications with the use of mTOR inhibitors for cancer therapy. Cancer Treat Rev 2014;40:190–6.
47. Slotkin EK, Patwardhan PP, Vasudeva SD, de Stanchina E, Tap WD, Schwartz GK. MLN0128, an ATP-competitive mTOR kinase inhibitor with potent in vitro and in vivo antitumor activity, as potential therapy for bone and soft-tissue sarcoma. Mol Cancer Ther 2015;14:395–406.
48. Welsh SJ, Corrie PG. Management of BRAF and MEK inhibitor toxicities in patients with metastatic melanoma. Ther Adv Med Oncol 2015;7:122–36.
49. Infante JR, Fecher LA, Falchook GS, Nallapareddy S, Gordon MS, Becerra C, et al. Safety, pharmacokinetic, pharmacodynamic, and efficacy data for the oral MEK inhibitor trametinib: a phase 1 dose-escalation trial. Lancet Oncol 2012;13:773–81.

Downloaded from http://aacrjournals.org/mct/article-pdf/18/11/1985/1859957/1985.pdf by guest on 28 August 2022